

Process Simulation and Evaluation of Carbon Separation Technology from High-CO₂ Gas Wells in Indonesia Using a Solvent and Adsorbent



Renanto Renanto^{1,*} , Tyara Novia Andhin¹ and Juwari Juwari¹

¹Department of Chemical Engineering, Faculty of Industrial Technology and Systems Engineering, Institut Teknologi Sepuluh Nopember, Surabaya, Indonesia

Abstract:

Background: With the global shift towards cleaner energy, natural gas demand is rising due to its lower environmental impact compared to oil. The gas reserves of Indonesia, notably in fields, such as Masela, Jambaran Tiung Biru (JTB), and Natuna, often have high CO₂ content. Effective CO₂ separation is vital to meet commercial gas standards while minimizing energy consumption.

Methods: This study evaluates the energy efficiency of two established CO₂ separation technologies: absorption using MEA solution and adsorption with a carbon molecular sieve. Both methods were simulated in Aspen software to assess energy requirements across different gas fields.

Results: Adsorption showed superior energy efficiency in all fields. For Masela (93% recovery), adsorption required 3.63E+03 GJ, significantly lower than absorption's 2.46E+04 GJ. In JTB (95% recovery), adsorption consumed 1.43E+03 GJ, outperforming absorption's 2.75E+04 GJ. For Natuna (93% recovery), adsorption used 1.37E+04 GJ versus absorption's 3.49E+05 GJ. CO₂ concentration emerged as a key factor in separation efficiency; adsorption was most effective at moderate CO₂ levels, such as JTB's 35%. However, low CO₂ levels (10%) in Masela reduced adsorption efficiency due to incomplete saturation, while high levels (71%) in Natuna led to rapid adsorbent saturation.

Conclusion: Adsorption demonstrated greater energy efficiency across varying CO₂ concentrations, though it performed best at medium levels. Absorption efficiency declined at higher CO₂ concentrations, limiting its suitability for gas fields with high CO₂ content. These findings highlight the potential of adsorption for more energy-efficient CO₂ separation in the gas fields of Indonesia.

Keywords: Absorption, Aspen, CO₂ separation, Gas processing, Gas Wells, Thermodynamic Model, Adsorbent.

© 2025 The Author(s). Published by Bentham Open.

This is an open access article distributed under the terms of the Creative Commons Attribution 4.0 International Public License (CC-BY 4.0), a copy of which is available at: <https://creativecommons.org/licenses/by/4.0/legalcode>. This license permits unrestricted use, distribution, and reproduction in any medium, provided the original author and source are credited.

*Address correspondence to this author at the Department of Chemical Engineering, Faculty of Industrial Technology and Systems Engineering, Institut Teknologi Sepuluh Nopember, Surabaya, Indonesia; E-mail: renanto@chem-eng.its.ac.id

Cite as: Renanto R, Andhin T, Juwari J. Process Simulation and Evaluation of Carbon Separation Technology from High-CO₂ Gas Wells in Indonesia Using a Solvent and Adsorbent. Open Chem Eng J, 2025; 19: e18741231367703. <http://dx.doi.org/10.2174/0118741231367703250212065934>



Received: November 12, 2024

Revised: December 20, 2024

Accepted: January 05, 2025

Published: February 20, 2025



Send Orders for Reprints to reprints@benthamscience.net

1. INTRODUCTION

The global energy demand is predicted to increase significantly in the coming years and is currently dominated by fossil fuels, including coal, oil, and gas [1]. However, this reliance on fossil fuels has led to a significant rise in CO₂ emissions, contributing to global climate change. To address this, a global energy transition toward renewable energy has emerged, aimed at reducing

CO₂ emissions in the atmosphere. During this transition era, natural gas plays a crucial role as a cleaner energy source across various sectors, such as power generation, industry, and transportation, emitting less CO₂ and offering higher energy efficiency compared to coal and oil.

To support the energy transition, natural gas exploration has been ramped up. According to the Global Energy Review 2019, international demand for natural gas

is expected to increase by 40% between 2018 and 2050. The composition of natural gas produced from wells is influenced by factors, such as location, type, depth of the deposits, and regional geology, according to Jasim *et al.* [2]. Raw natural gas primarily contains methane (CH₄) along with smaller amounts of ethane, propane, butane, and heavier hydrocarbons, as well as non-hydrocarbon components like carbon dioxide (CO₂), hydrogen sulfide (H₂S), water (H₂O), nitrogen (N₂), and other residual components. The purification of raw natural gas is necessary to meet pipeline specifications and environmental regulations, according to da Cunha *et al.* [3].

Natural gas processing typically involves four main steps: pretreatment, acid gas removal, dehydration, and liquefaction. Pretreatment removes unwanted substances through separation units that are also capable of separating gas from oil and water phases. Before further processing in dehydration and liquefaction units, acid gases, such as H₂S and CO₂, must be removed using separation processes, according to Poe and Mokhtab [4]. The presence of CO₂ in natural gas, particularly when combined with water, can cause corrosion in pipelines and equipment, reduce the calorific value of the gas, and even lead to crystallization during the liquefaction process, according to Nasir and Iran [5].

However, significant challenges remain, particularly due to the high variability in CO₂ content in natural gas reservoirs, which complicates separation and purification processes. Significant variations in CO₂ content have been observed in natural gas worldwide, with CO₂ levels ranging from 4% to 50% in raw natural gas and even reaching 71% in some cases, such as in the Natuna gas field, according to Murbini [6]. While high CO₂ content in natural gas poses processing difficulties, it also presents opportunities for utilization, such as enhanced oil or gas recovery or underground storage. Although these applications fall outside the scope of this paper, they have been addressed in other studies.

The variation in composition, pressure, and temperature of natural gas determines the most suitable carbon removal technology, as noted by Iran & Chem [5]. No single technology is ideal for all conditions, so an effective process design should consider various technologies and select the most efficient option [7]. Although several evaluation and analysis studies have investigated these processes separately or compared them for specific applications, specific assessments of absorption and adsorption for high-CO₂ gas wells are scarce in the literature. The study by Anselmi *et al.* [8] compared the three CO₂ separation technologies, but with a maximum CO₂ content of 9%, focusing on air-CO₂ separation. They found that absorption had the highest recovery and purity levels, although it also had the highest energy consumption.

Therefore, the novelty of this study lies in the comparative evaluation of solvent- and adsorbent-based CO₂ separation technologies, specifically applied to the

high-CO₂ gas wells of Indonesia, characterized by their distinct composition and operating conditions. By simulating both technologies in Aspen, the study identifies adsorption as the more energy-efficient method across all fields, highlighting its superior performance at medium CO₂ concentrations. This comparative analysis offers new insights into optimizing CO₂ separation technology based on field-specific gas composition, which is critical for enhancing energy efficiency in Indonesia's growing natural gas sector.

2. GAS FIELD DATA

This study uses data from three natural gas fields in Indonesia, each with different compositions and operating conditions, as outlined in Table 1, to determine which technology is most suitable for each set of operating conditions.

Table 1. Operating condition of natural gas in three different fields [9, 10, 11].

Gas Field	Flowrate (MMSCFD)	Pressure (bar)	Temperature (°C)
Masela	1200	51	103
Jambaran Tiung Biru	340	42	100
Natuna	2353	68	40

Since the dominant components in natural gas composition are CH₄ and CO₂, the simulation for absorption and adsorption can assume that the feed gas is a binary mixture. This simplification to a binary mixture is also intended to reduce the complexity of the adsorption simulation, allowing the use of a single adsorbent layer. The normalized gas composition and flow rates, which will serve as the inlet parameters for the absorption and adsorption simulations, are shown in Table 2.

Table 2. Normalized natural gas composition in three different fields.

	Masela	JTB	Natuna
Feed Comp	Mole %	Mole %	Mole %
CH ₄	89.77	63.15	27.46
CO ₂	10.23	36.85	72.54
Flowrate (kmol/h)	54257	16126	115203
Athor/Reference	Amalia Handini Astari in [9]	Nizami <i>et al.</i> in [10]	Anugraha <i>et al.</i> in [11]

3. METHODOLOGY ABSORPTION SIMULATION MODEL

3.1. Absorption and Thermodynamic Model

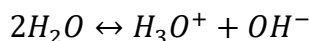
The most common and proven method for removing CO₂ is through the absorption process in a solvent containing amine, followed by desorption. The simplest and most used amine for CO₂ removal is MEA (monoethanolamine). In its application, MEA concentration is limited to 30% due to its corrosive nature.

In the study by Luo and Wang [12], the PC-SAFT EOS was used to calculate vapor phase properties, and the

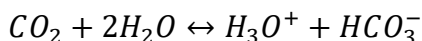
eNRTL method was used to model the electrolyte system of the MEA-H₂O-CO₂ mixture. Most of the eNRTL model parameters used in that study were obtained from the SRK-ASPEN databank, and some were updated by recent studies through regression using new experimental data.

The liquid-phase chemical reactions involved in the MEA-H₂O-CO₂ system can be expressed as follows:

R1: water dissociation



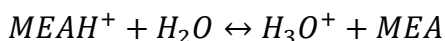
R2: dissociation of CO₂



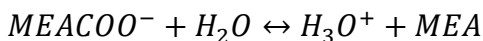
R3: dissociation of carbonate



R4: dissociation of the protonated amine



R5: carbonate formation



The traditional method for modeling absorption columns is by using equilibrium methods. Each stage can be calculated by assuming equilibrium between the CO₂ concentrations in the gas and the liquid leaving that stage. This equilibrium stage model can be represented with efficiency for each stage. The Murphree efficiency for stage number n is defined in Eq-1 as follows.

$$E_M = \frac{y - y_{n-1}}{y^* - y_{n-1}} \quad (1)$$

where y is the mole fraction of CO₂ in the gas leaving the stage, Y_{n-1} is the mole fraction leaving the stage below, and y* is the mole fraction of CO₂ in equilibrium with the liquid leaving the stage. Most process simulation programs have a model for applying Murphree efficiency in column modeling. Aspen HYSYS has a specific estimation method for predicting Murphree efficiency, which is based on experience with CO₂ removal from high-pressure natural gas.

3.1. Operating Condition

Gas streams containing a target component (e.g., CO₂) are passed through an absorption column where it contacts a liquid absorbent. The target component dissolves in the liquid, effectively removing it from the gas stream. The rich absorbent (now containing the absorbed target component) is then heated or otherwise treated in a regeneration unit to release the absorbed component. This step separates the target component from the absorbent, allowing the absorbent to be recycled for reuse. The process flow diagram typically includes the main units for

acid gas removal, namely the absorption column, heat exchanger, and regeneration column, as illustrated in Fig. (1).

The fixed operating conditions for the three gas fields are presented in Table 3. The remaining details will be discussed in the following section.

Table 3. Operating condition of absorber and stripper in HYSYS.

Absorber	
Column pressure (kPa)	5617
Gas temperature (°C)	38
Gas pressure (kPa)	5686
Lean amine temperature (°C)	43,33
Lean amine pressure (kPa)	5686
Lean amine concentration (%mol)	30
Stripper	
Overhead pressure (kPa)	110
Bottomhead pressure (kPa)	120

3.2. Energy and Recovery

The absorber performance is represented by CO₂ recovery, which indicates how much CO₂ from the feed gas can be removed during the absorption process. CO₂ recovery is defined as the amount of CO₂ in the product gas compared to the amount of CO₂ in the feed gas, as shown in the following equation 2:

$$\%CO_2 \text{ Recovery} = \left(1 - \frac{\text{Amount of } CO_2 \text{ in product (kmol)}}{\text{Amount of } CO_2 \text{ in feed (kmol)}}\right) \times 100\% \quad (2)$$

In addition to CO₂ recovery, energy consumption is another critical parameter for evaluating the performance of different technologies. To compare it with adsorption, it is necessary to standardize the units expressed in kJ based on a 2400-second time frame, which corresponds to the duration of the adsorption cycle. as shown in eq 3 and 4:

$$\Sigma \text{Energy Consumption} = \Sigma \text{Thermal} + \Sigma \text{Work} \quad (3)$$

$$\Sigma \text{Energy Consumption (kJ)} = (\Sigma \text{Condenser} + \Sigma \text{Reboiler} + \Sigma \text{Cooler}) + (\Sigma \text{pump}) \quad (4)$$

4. ADSORPTION SIMULATION MODEL

4.1. Pressure Swing Adsorption

Pressure Swing Adsorption (PSA) is a cyclic adsorption process primarily designed for gas separation and purification, and it is widely used for gas separation. Industrial processes typically employ more than one pair of adsorption and desorption columns operating in parallel. The Pressure Swing Adsorption (PSA) process involves multiple stages, where pressure changes within the adsorption bed, the duration of each stage, and the sequence of valve operations vary according to Hosseini and Denayer [13].

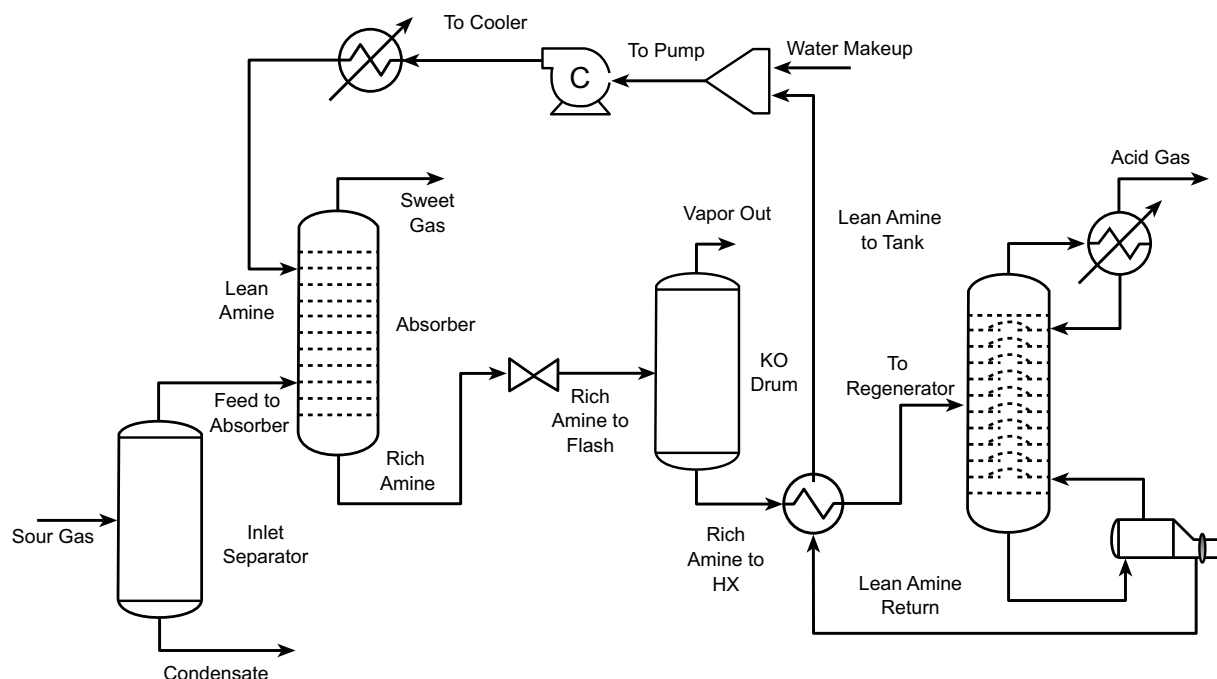


Fig. (1). CO₂ absorption process flow diagram.

First, gas flows into the adsorption column (Bed1) and increases the pressure to the desired level (PR). The process enters the adsorption stage (AD), where the second adsorption column (Bed2) contains more CO₂, and the stream leaving Bed1 has a low CO₂ concentration (high CH₄ content). Then, part of the CH₄ product is transferred to Bed2 to assist in adsorbent regeneration. After that, Bed1 becomes saturated, and Bed2 is regenerated. The process then proceeds with the depressurization equalization step (DPE), which is crucial for reducing energy consumption by minimizing gas compression. After this step, the process is repeated with the roles of the two adsorption beds reversed, as shown in Fig. (2). This basic process includes the following six steps:

1. Pressurization (PR);
2. Adsorption (AD);
3. Depressurization equalization (DPE);
4. Blowdown (BL);
5. Purging (PU);
6. Pressure equalization (PPE).

The Pressure Swing Adsorption (PSA) simulation using a dual bed, as shown in Fig. (3), was conducted using Aspen Adsorption. To represent the dual bed, the interacting single bed full flowsheet approach can be employed to simulate the complete cyclic system of interacting units. This approach is valid under the following assumptions:

- Each adsorbent layer is identical
- Only one adsorbent layer needs to be modeled accurately
- A set number of interactions can be applied
- The material transferred to the interacting bed is reused (replayed) within the cycle

4.2. Simulation Flowsheet

4.2.1. Adsorber and Adsorbent Specifications

The adsorbent material is crucial to the PSA unit. All cycle properties (operating conditions and modes) depend on the initial choice of adsorbent. A study from Djeridi [15] has demonstrated that not only the micropore volume but also the structural, textural, and electrical characteristics affect CO₂ adsorption capacity. Several materials can be used in PSA technology, and the selected material must meet at least one of two criteria:

- The material must have a higher selectivity for CO₂. This type of material is referred to as an equilibrium-based adsorbent because its selectivity is mainly due to differences in interaction forces between CO₂ and CH₄ with the surface.
- Adsorbent pores can be arranged to allow CO₂ (kinetic diameter 3.4 Å) to easily penetrate their structure. This material is known as a kinetic adsorbent because its selectivity is primarily due to diffusion constraints. Carbon molecular sieves (CMS) are among the most widely used materials for CO₂ separation.

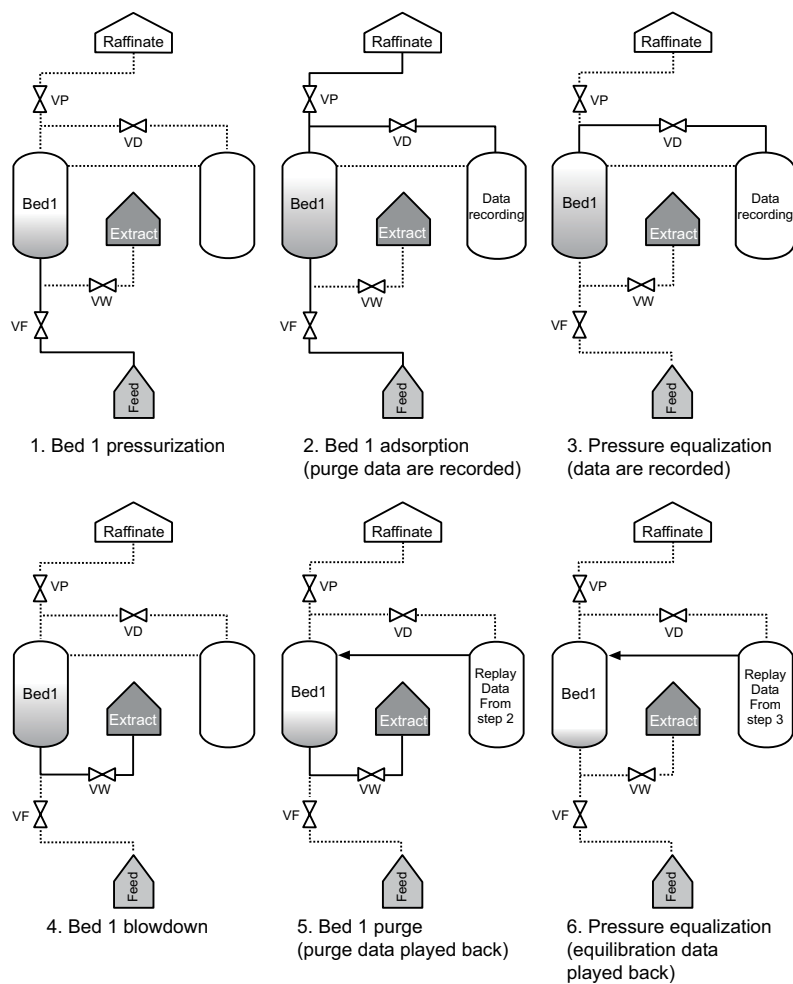


Fig. (2). Six steps of pressure swing adsorption (PSA) cyclic according to Kottitum *et al.* in [14].

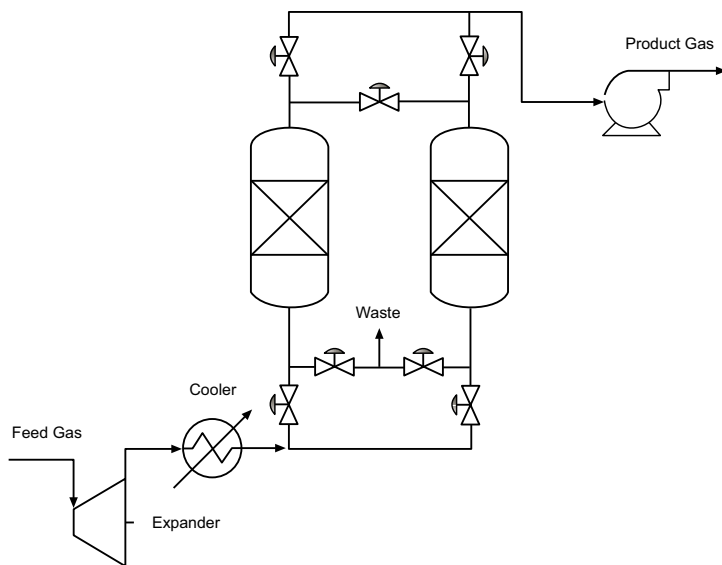


Fig. (3). CO₂ adsorption process flow diagram.

The adsorption equilibrium isotherms for CO₂ and CH₄ in CMS-3K are shown in Fig. (4). While this material clearly has selectivity for CO₂, the most important property of CMS-3K is not its equilibrium selectivity, but its kinetic selectivity according to Grande [16].

Grande and Rodrigues have studied the performance of CMS-3K adsorbent in a five-step process compared to zeolite adsorbent in a four-step process. The results show that both adsorbents achieved CH₄ purity above 98%, but the CH₄ recovery with CMS-3K was higher than with zeolite, reaching 80% compared to 60% for zeolite. The molecular-sized pores in CMS provide high kinetic selectivity and adsorption capacity for various gases. Therefore, CMS was selected for this study based on the parameters provided in Table 4, as described by Kottitum *et al.* [14].

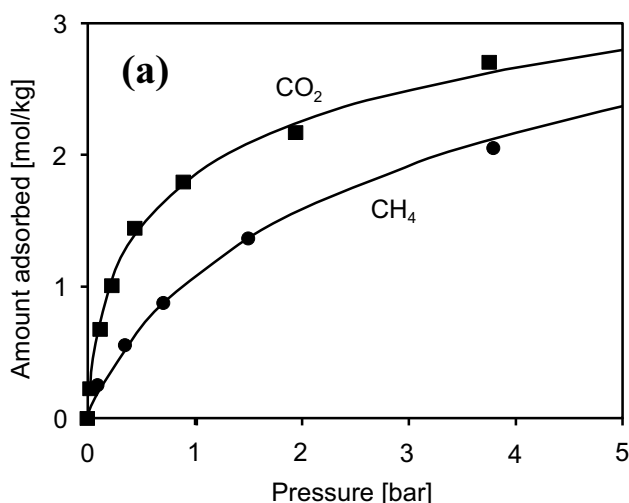
Table 4. Physical properties of CMS-3K [14].

Parameter Name	Value	Unit
Adsorbent bulk solid density	715.93	kg/m ³
Adsorbent particle radius	9e-04	m
Porosity	0.33	-

The isotherm parameter values were obtained from experimental data by Kottitum *et al.* [14], and the Langmuir isotherm equation is provided in Table 5.

Table 5. Parameter langmuir isotherm [14].

Description	IP1 (x10 ⁻⁶)	IP2	IP3	IP4
CH ₄	6.31	1056	4.7e-05	1067
CO ₂	12.7	1187	1.23e-04	1210



Mass transfer coefficients and the equilibrium adsorption model are key parameters for validating the modeling results with experimental data. In this study, the values obtained from the simulation by Kottitum *et al.* [14] are used, and the corresponding values can be found in Table 6, along with several other parameters.

4.3. Adsorption Isotherm

The most found in the literature is the Langmuir isotherm, which also serves as the basis for other types of isotherms. The Langmuir isotherm is one of the simplest models available to represent the interaction between adsorbent and adsorbate. The Langmuir equation (5) is given as:

$$q = \frac{q_s b p_i}{1 + b p_i} \quad (5)$$

Where:

- q is the adsorption capacity, in kmol/kg,
- p_i is the partial pressure of the component
- q_s is the maximum adsorption capacity in kmol/kg,
- b is the Langmuir parameter in bar

Various extensions and advanced versions of the Langmuir isotherm have been developed to be applied in different situations. For instance, the Extended Langmuir is often used for multicomponent systems. The Langmuir variation applied in Aspen Adsorption is provided in Table 7, where the fitting parameters are denoted with the notation IP. Further details on this equation can be found in the help section of the simulation software, according to Maksimov, [17].

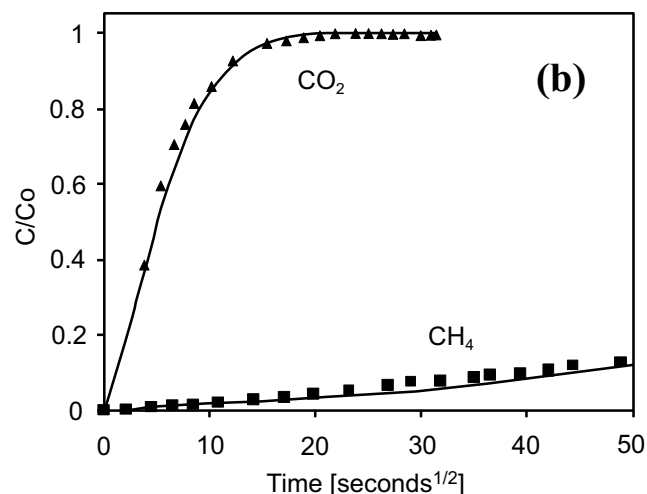


Fig. (4). CO₂ and CH₄ adsorption in 3K carbon molecular sieve at 298 K: (a) adsorption equilibrium; (b) absorption rate curve according to Grande in [16]

Table 6. Adsorbent parameter.

Parameter	Value	Unit	Description
MTC (*)			
MTC ("CH ₄ ")	5	1/s	Constant mass transfer coefficients
MTC ("CO ₂ ")	110	1/s	Constant mass transfer coefficients
Dm (*)			
Dm ("CH ₄ ")	6,70E-05	m ² /s	Molecular diffusivity
Dm ("CO ₂ ")	5,65E-05	m ² /s	Molecular diffusivity
Cps	1,00E-03	MJ/kg/K	Adsorbent-specific heat capacity
Cpa (*)			
Cpa ("CH ₄ ")	0,0365	MJ/kmol/K	Constant adsorbed phase heat capacities
Cpa ("CO ₂ ")	0,0375	MJ/kmol/K	Constant adsorbed phase heat capacities
DH (*)			
DH ("CH ₄ ")	-18	MJ/kmol	Constant for the heat of adsorption
DH ("CO ₂ ")	-24,6	MJ/kmol	Constant for the heat of adsorption
HTC	1	MW/m ² /K	Constant for the heat transfer coefficient
Kg	2,50E-08	MW/m/K	Constant for the gas phase heat conductivity
Ks	6,00E-07	MW/m/K	Adsorbent thermal conductivity
ap	2057,14	1/m	Specific surface area of the adsorbent

Table 7. Isotherm langmuir variation [17].

Isotherm Variation	Isotherm Equation
Langmuir 1	$q = \frac{IP_1 p_i}{1 + IP_2 p_i} \quad (6)$
Langmuir 2	$q = \frac{IP_2 \exp \frac{IP_2}{T_s} p_i}{1 + IP_3 \exp \frac{IP_4}{T_s} p_i} \quad (7)$
Langmuir 3	$q = \frac{(IP_1 - IP_2 T_s) IP_3 \exp \frac{IP_4}{T_s} p_i}{1 + IP_3 \exp \frac{IP_4}{T_s} p_i} \quad (8)$
Extended Langmuir 1	$q = \frac{IP_{1i} p_i}{1 + \sum_k (IP_{2k} p_k)} \quad (9)$
Extended Langmuir 2	$q = \frac{IP_{1i} \exp \frac{IP_{2i}}{T_s} p_i}{1 + \sum_k (IP_3 \exp \frac{IP_{4k}}{T_s} p_k)} \quad (10)$
Extended Langmuir 3	$q = \frac{(IP_{1i} - IP_{2i} T_s) IP_{3i} \exp \frac{IP_{4i}}{T_s} p_i}{1 + \sum_k (IP_3 \exp \frac{IP_4}{T_s} p_k)} \quad (11)$

4.4. Mathematic Model

In this study, the Peng-Robinson model was selected due to its suitability for non-ideal gas phases and its widespread use in CO₂/CH₄ separation via the PSA (Pressure Swing Adsorption) technique according to Kottitum *et al.* [14]. Meanwhile, the adopted momentum balance is based on the Ergun equation 12, which is expressed as follows:

$$\frac{\partial P}{\partial z} = \frac{1.5 \cdot 10^{-3} \mu (1-\varepsilon)^2}{d_p^2 \varepsilon^2} U + \frac{1.75 \cdot 10^{-5} \rho_g (1-\varepsilon)}{d_p \varepsilon} U^2 \quad (12)$$

In this study, the Extended Langmuir 2 model was used, expressed as a function of the partial pressures of various components, as presented in Aspen Adsorption, and capable of accounting for temperature dependence. Meanwhile, the energy equilibrium model used is the non-isothermal model with gas and solid conduction Kottitum *et al.* [14].

In this case, a lumped resistance model with a linear form was chosen, which simplifies the analysis by considering only one resistance per component. Therefore, as previously mentioned, the analysis was simplified by using a single kinetic parameter for CH₄ and CO₂. This kinetics model was adjusted using the linear driving force model, which is commonly applied in kinetic studies shown in eq 13.

$$\frac{\partial q_i}{\partial t} = K_i (q_i^* - q_i) \quad (13)$$

4.5. Cycle Organizer

To create a cyclically operated process, a tool called Cycle Organizer can be used in the simulation with Aspen Adsorption. In this study, it is necessary to set the time for each stage (control variable), as shown in Table 8.

Table 8. 6 steps duration of pressure swing adsorption (PSA) cyclic.

Step	Duration (s)
Adsorption	40
Depressurization	10
Blowdown	10
Purge	40
Repressurization	10
Pressurization	10

In addition to setting the time in the Cycle Organizer, manipulated variables must also be specified. These variables include the valve opening and closing settings, as well as the valve specifications. The valve operation schedule is arranged using the numbering system, as shown in Table 9.

Table 9. Valve specification for controlling.

Step	Position
0	Fully closed valve (flow rate through the valve is always zero)
1	Fully open valve (flow rate through the valve will be determined by mass balance)
2	Flow rate through the valve will have a linear relationship with pressure drop
3	Valve will have a constant flow rate

4.6. Energy and Recovery

The performance of the adsorber is represented by CO₂ recovery, which indicates how much CO₂ from the feed gas can be removed during the adsorption process. CO₂ recovery is defined as the amount of CO₂ in the product gas compared to the amount of CO₂ in the feed gas, as shown in the following equation:

$$\%CO_2 \text{ Recovery} = \left(1 - \frac{\text{Amount of } CO_2 \text{ in product (kmol)}}{\text{Amount of } CO_2 \text{ in feed (kmol)}}\right) \times 100\% \quad (14)$$

In addition to CO₂ recovery, which is a key performance parameter in this experiment, energy consumption is also an important parameter for evaluating the effectiveness of the technology.

$$\text{Energy Consumption} = \Sigma \text{Thermal} + \Sigma \text{Work} \quad (15)$$

$$\Sigma \text{Energy Consumption (kJ)} = (\Sigma \text{Cooler}) + (\Sigma \text{Compressor}) \quad (16)$$

5. RESULTS AND DISCUSSION

5.1. Absorption using Aspen HYSYS

This flowsheet is used to simulate data from the three gas fields involved in the study, as shown in Fig. 5. However, adjustments in pressure and temperature are made before the gas enters the absorber column, which is designed for a pressure of 51 bar and a temperature of

approximately 40°C. Although the flowsheet for the three gas fields appears similar, the design specifics, such as the number of trays and the solvent used, will be adjusted according to the conditions of each field to achieve recovery values comparable to those of other technologies, such as adsorption. Additionally, it is crucial to ensure that the temperature of the liquid product from the absorber, which contains MEA, does not exceed 120°C to prevent degradation.

With varying CO₂ compositions in the three gas fields, adjustments are made to the absorber operating conditions, such as the number of trays and the amount of solvent for each field, as shown in Table 10. There is a relationship between CO₂ concentration, solvent amount, and the outlet temperature of the amine (rich amine). Since the reaction between CO₂ and amine solvent is exothermic, a higher CO₂ concentration leads to a higher temperature of the product exiting the absorber. This can be mitigated by increasing the amount of solvent, which lowers the outlet temperature of the absorber. As explained, the temperature of the rich amine must be maintained around 120°C to prevent degradation. For more details, the operating conditions of the absorber and stripper are provided in Table 10.

Before applying the model to scenarios with relevant CO₂ concentrations, a preliminary simulation based on the work of Wang *et al.* [18] was conducted to validate the assumptions outlined earlier. Wang *et al.* [18] studied CO₂ absorption using MEA and validated their model using real operational data.

After making several adjustments, the CO₂ recovery values achieved are as follows: for the Masela field, CO₂ recovery is 93% with CH₄ purity at 99%; for the JTB field, CO₂ recovery is 95.43% with CH₄ purity at 97.24 mol%; and for the Natuna field, CO₂ recovery is 93.68% with CH₄ purity at 85.2 mol%. From the absorption process, the energy consumption is detailed in Table 11. The highest energy usage is observed in the condenser and reboiler, which are part of the stripper. As the separation process in the stripper becomes more efficient and the amount of solvent increases, the energy consumption also rises.

Table 10. Operating condition for absorber column in three different fields.

Absorber	Masela	JTB	Natuna
Number of tray	20	18	17
Solvent (kmol/h)	61195	68540	881200
Rich Amine temperature (°C)	121.8	117	123
Rich Amine pressure (kPa)	5617	5617	5617
Sweet Gas temperature (°C)	45.37	45.37	44.34
Sweet Gas pressure (kPa)	5617	5617	5617
Stripper			
Number of trays	10	10	8
Reboiler temperature (°C)	175	175	175
Condenser temperature (°C)	98	98	98

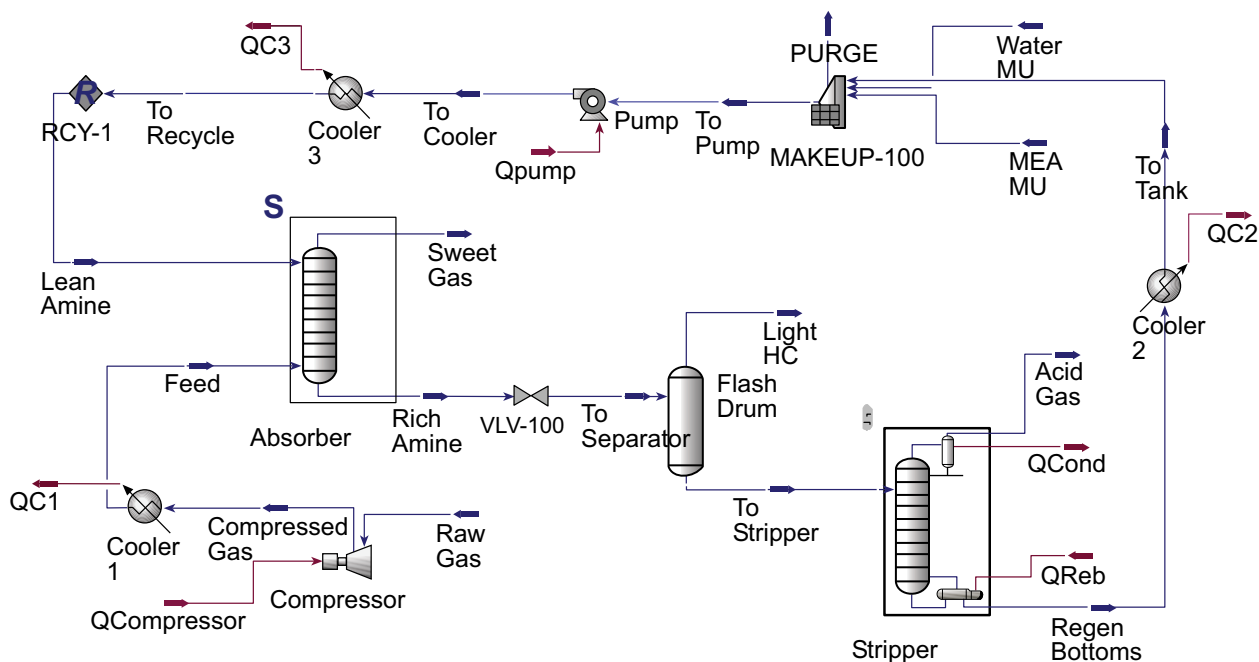


Fig. (5). CO₂ absorption process flow diagram in ASPEN HYSYS.

Table 11. Energy consumption of the absorption process in the masela gas field.

Energy (kJ)	Reboiler	Condenser	Pump	Cooler 1	Cooler 2	Cooler 3
Masela	1.73E+10	1.89E+10	9.79E+06	1.31E+08	1.68E+08	3.56E+08
JTB	1.93E+10	2.12E+10	1.10E+07	4.57E+07	1.88E+08	3.99E+08
Natuna	2.46E+11	2.70E+11	1.41E+08	4.71E+07	2.42E+09	5.12E+09

5.2. Adsorption using Aspen Adsorption

In the simulation, a PSA approach with a single bed is used, as shown in Fig. 6, with the composition and flow rates adjusted according to the natural gas conditions produced by each field. In the PSA cycle, adsorption occurs at a pressure of 10 bar, while purging takes place at a pressure of 6 bar.

In this study, a single PSA cycle using dual beds consists of 6 steps controlled by valves. These valves can be adjusted using the Cycle Organizer, with specifications provided in Table 12. The use of these 6 steps is expected to help reduce energy consumption.

The adsorption simulation is conducted by dividing the feed gas flow rate, as in real-world applications where adsorption is arranged in parallel with multiple pairs of PSA beds. The recovery value in the adsorption process is influenced by several factors, such as the type of adsorbent and the duration of adsorption. Longer adsorption durations result in greater CO₂ absorption by the adsorbent; however, there is a limit to the adsorbent's capacity to absorb CO₂ due

to saturation levels. Further information about the operating condition of the adsorption column is shown in Table 13.

To ensure the accuracy of the assumptions described above, a preliminary simulation was conducted for validation before applying the model to scenarios with relevant CO₂ concentrations. The validation is based on the work of Kottitum [14], which investigated adsorption for biogas purification and validated their model using real operational data.

Before entering the adsorption bed, the feed gas undergoes pretreatment to reduce the temperature and pressure to 25°C and 10 bar. The total energy consumed during the PSA process to achieve CO₂ recovery values of 93% for the Masela field, 95.15% for the JTB field, and 93.06% for the Natuna field is noted. The energy required for regeneration in this process is significantly lower compared to solvent regeneration in absorption, as shown in Table 14. This value will increase with higher CO₂ absorption and when aiming for higher recovery values.

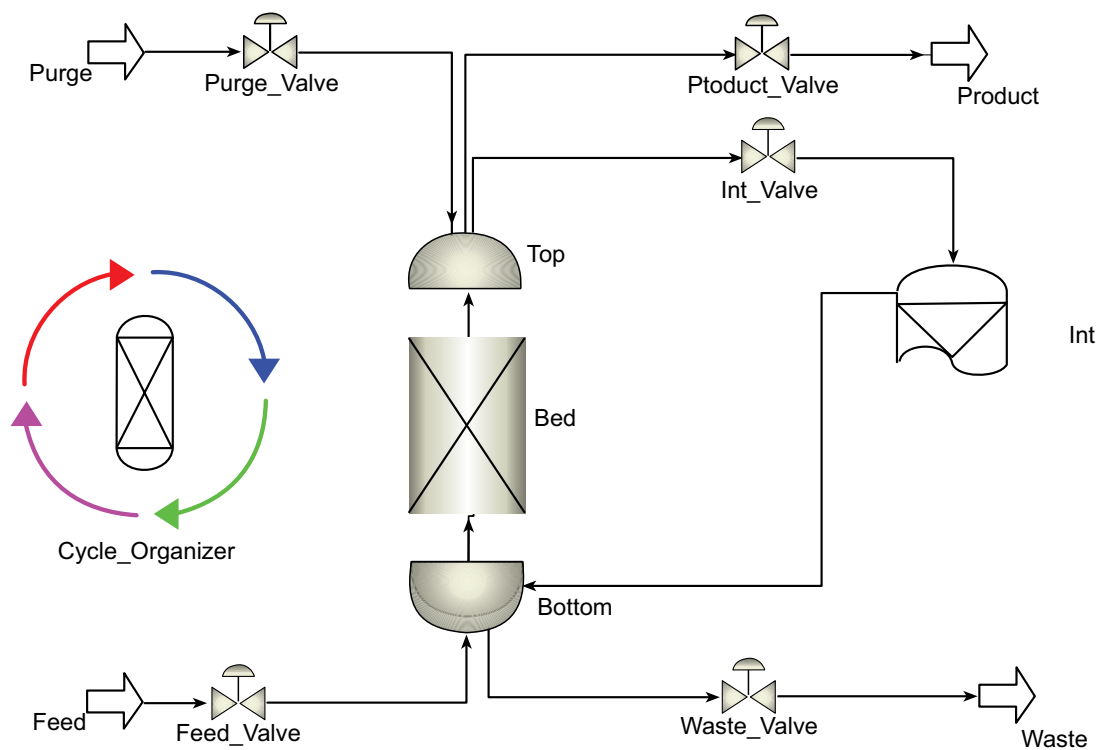


Fig. (6). CO₂ adsorption process flow diagram in aspen adsorption.

Table 12. Valve controlling of PSA 6 step.

Step	Function	Valve				
		Feed	Product	Int	Waste	Purge
Step 1	Absorption bed 1, purge bed 2	3	1	0	0	0
Step 2	DPE bed 1, RPE bed 2	0	0	2	0	0
Step 3	Blowdown bed 1, pressurization bed 2	0	0	0	2	0
Step 4	Purge bed 1, adsorption bed 2	0	0	0	1	3
Step 5	RPE bed 1, DPE bed 2	0	0	2	0	0
Step 6	Pressurization bed 1, blowdown bed 2	2	0	0	0	0

Table 13. Operating condition of adsorption column.

Step	Pressure (bar)	Temperature (°C)	Energy (kJ)
Adsorption	10	25	$W=nR(T1)\ln(P1/Pfeed)$
Depressurization	10 to 5	25 to 12	0 (conserves by equalizing)
Blowdown	5 to 1	12 to (-7)	$W=nR(T2)\ln(P3/P2)$
Purge	1	(-7)	$W=nR(T3)\ln(Ppurge/P3)$
Repressurization	1 to 5	(-7) to 10	0 (conserves by equalizing)
Pressurization	5 to 10	10 to 25	$W=nR(T5)\ln(P6/P5)$

5.3. Energy Comparison of Absorption and Adsorption for Each Field

From the simulation results of CO₂ separation for the Masela, Jambaran Tiung Bitu, and Natuna gas fields, it is observed that adsorption technology performs better in terms of energy consumption compared to absorption technology, as shown in Table 15. These findings are supported by Zanco *et al.* [7], who stated that among absorption, adsorption, and membrane technologies for a 12% CO₂ feed, absorption has higher energy consumption. However, this comparison is based solely on energy consumption, and the results may differ when considering the costs associated with both technologies. According to Zanco *et al.* [7], while adsorption offers lower energy consumption and can handle relatively high CO₂ concentrations, its application is typically limited to small-scale plants. In contrast, absorption, despite its higher energy consumption, has been proven effective in several large-scale plants. Therefore, it is important to note that a comprehensive evaluation should also include cost analysis, which will be addressed in future work.

Table 15 also shows that although the Masela field has a CO₂ concentration of 10% and a flow rate of 1200 MMSCFD, and the JTB field has a CO₂ concentration of 35% and a flow rate of 340 MMSCFD, the energy consumption for CO₂ separation from natural gas in both fields can be similar. This is due to the total mass of CO₂ that needs to be removed from the gas stream being nearly identical in both fields. The Masela field, despite having a lower CO₂ concentration, processes a significantly larger gas volume, resulting in a substantial total mass of CO₂. Conversely, the JTB field, with a higher CO₂ concentration but a lower flow rate, also produces a comparable total mass of CO₂. Thus, the energy required

for CO₂ separation in both fields is almost the same despite differing operational conditions and CO₂ concentrations.

5.4. Effects of CO₂ Concentration, Pressure, and Temperature

The three gas fields used in this study exhibit different operating conditions in terms of CO₂ concentration, temperature, flow rate, and pressure. However, among these four variables, CO₂ concentration has the most significant influence on determining the CO₂ separation technology. Therefore, an analysis was conducted to assess the impact of CO₂ concentration on the separation performance (recovery) of the absorber and adsorber.

To ensure a fair comparison, simulations were performed with the same flowrate, pressure, and temperature for all three fields. The selected conditions were a flowrate of 340 MMSCFD, pressure of 51 bar, and temperature of 40°C. Additionally, the operating conditions of each piece of equipment within the CO₂ separation unit were kept constant, ensuring that the energy consumption across the fields remained comparable. This approach provides a clearer understanding of how varying CO₂ concentrations influence the performance of both absorption and adsorption processes.

On the other hand, from the absorber simulation using Aspen Adsorption, the performance of the absorber for the three fields is shown in Fig (7). It was concluded that the adsorber performed best in the JTB field with a gas concentration of 35%. For the Masela gas field with 10% CO₂, the performance was the lowest, followed by the Natuna gas field with 71% CO₂. This is due to the characteristics of the adsorbent, which has an optimal capacity at medium concentrations, like in the JTB field.

Table 14. Energy consumption of adsorption in three different fields.

Energy (kJ)	Feed Cooler	Compressor PSA	Total
Masela	1.97E+08	3.43E+09	3.63E+09
JTB	1.38E+09	5.44E+07	1.43E+09
Natuna	1.36E+10	1.10E+08	1.37E+10

Table 15. CO₂ recovery and energy consumption of absorption and adsorption in three different fields.

Field	%CO ₂	Temperature	Pressure	Flowrate	CO ₂ recovery		Energy Consumption (kJ)	
					Absorption	Adsorption	Absorption	Adsorption
Masela	10,23	103 (°C)	51 bar	1200 MMSCFD	93%	93%	2,46E+10	3,63E+09
JTB	36,85	100 (°C)	42 bar	340 MMSCFD	95,43%	95,15%	2,75E+10	1,43E+09
Natuna	72,54	40 (°C)	68 bar	2353 MMSCFD	93,68%	93,06%	3,49E+11	1,37E+10

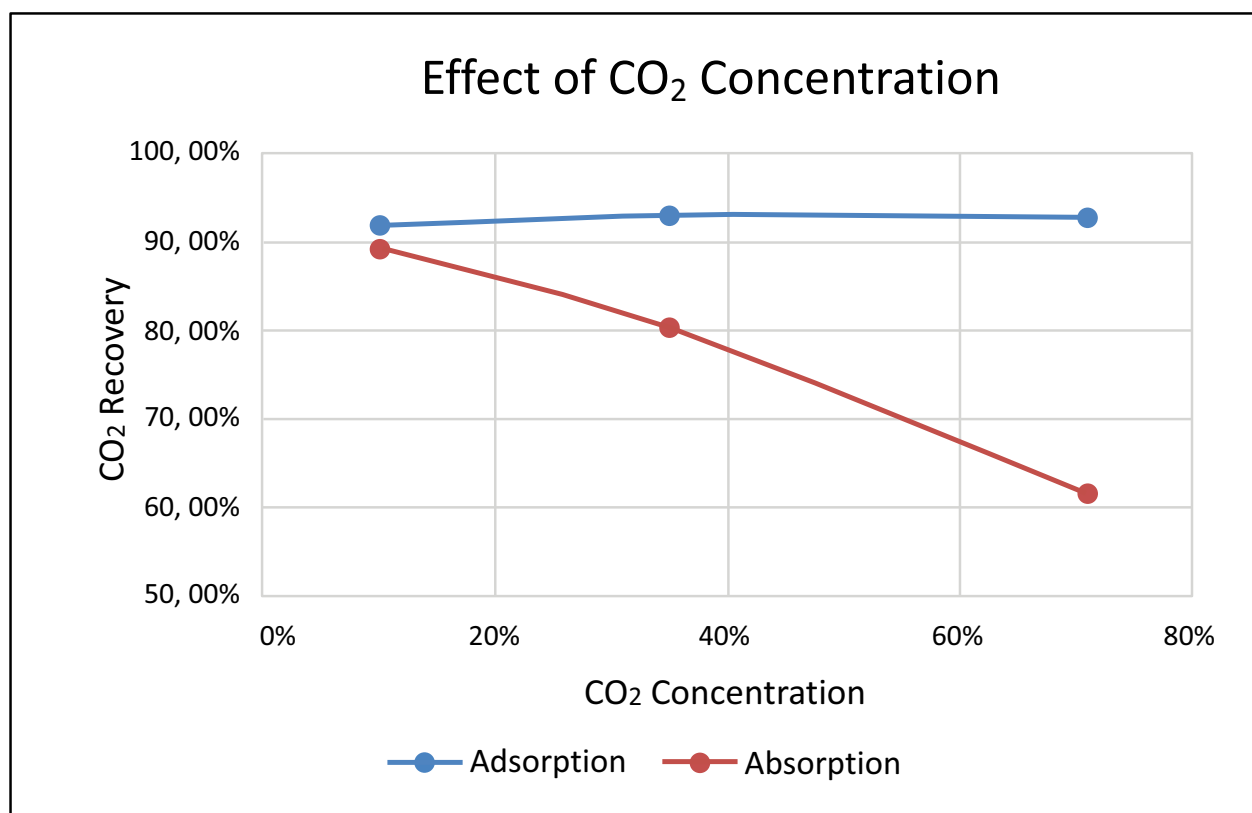


Fig. (7). CO₂ concentration effect on absorption and adsorption performance.

At low concentrations, such as in the Masela field, the adsorbent does not work as efficiently because there is insufficient gas to reach optimal saturation. Meanwhile, at very high concentrations, such as in the Natuna field, the adsorbent quickly reaches its saturation point, reducing the efficiency of further CO₂ adsorption. This highlights how the performance of the adsorber is strongly influenced by the concentration of CO₂, with mid-range concentrations providing the best balance between adsorption efficiency and gas availability.

To validate the results of the CO₂ separation technologies, the simulation outcomes were compared with previous studies and experimental data. The effect of CO₂ concentration on recovery rates in absorption and adsorption processes was evaluated against comparable studies by Mustafa *et al.* [19] for the absorption study and Kottitum *et al.* [14] for the adsorption study, which reported consistent trends.

CONCLUSION

In this study, simulations were conducted for carbon separation from the Masela, Jambaran Tiung Biru (JTB), and Natuna gas fields using absorption technology with Aspen HYSYS and adsorption technology with Aspen Adsorption. CO₂ separation in the Masela, JTB, and Natuna gas fields was found to be more suitable using adsorption technology due to its superior energy performance

compared to absorption. For both technologies at Masela field with 93% recovery, energy consumption for absorption was 2.46E+10 kJ, and for adsorption, it was 3.63E+09 kJ. At JTB with 95% recovery, absorption and adsorption consumed 2.75E+10 kJ and 1.43E+09 kJ, respectively. Meanwhile, at Natuna, with 93% recovery, absorption and adsorption consumed 3.49E+11 kJ and 1.37E+10 kJ, respectively. This research also highlighted that CO₂ concentration is the most influential variable in CO₂ separation, compared to temperature, pressure, and flowrate, which can be adjusted through pre-treatment. Aspen HYSYS simulations showed that absorber performance decreases with increasing CO₂ concentration due to mass load and rapid solvent saturation. Conversely, Aspen Adsorption simulations revealed that adsorbents work optimally at medium concentrations (35% CO₂) like in the JTB field. Low concentrations (10% CO₂) in the Masela field do not reach optimal saturation, and high concentrations (71% CO₂) in the Natuna field cause rapid saturation of the adsorbent, reducing adsorption efficiency.

AUTHORS' CONTRIBUTIONS

The authors confirm their contribution to the paper as follows: Study conception and design were contributed by R.R. and J.J.; and the manuscript was drafted by T.N.A. All authors reviewed the results and approved the final version of the manuscript.

LIST OF ABBREVIATIONS

CH ₄	=	methane
CO ₂	=	carbon dioxide
H ₂ S	=	hydrogen sulfide
H ₂ O	=	water
N ₂	=	nitrogen
PSA	=	Pressure Swing Adsorption
DPE	=	Depressurization equalization step
BL	=	Blowdown
PU	=	Purging
PPE	=	Pressure equalization
CMS	=	Carbon molecular sieves

CONSENT FOR PUBLICATION

Not applicable

AVAILABILITY OF DATA AND MATERIALS

The data and supportive information are available within the article.

FUNDING

This work was funded by [KEMENDIKBUDRISTEK] under the Hibah Penelitian Disertasi Doktor (PDD) [number 038/E5/PG.02.00.PL/2024] or [DRPM Institut Teknologi Sepuluh Nopember][number 1719/PKS/ITS/2024], Indonesia.

CONFLICT OF INTEREST

The authors declare no conflict of interest, financial or otherwise.

ACKNOWLEDGEMENTS

Declared none.

REFERENCES

- [1] J. Krzywanski, W.M. Ashraf, T. Czakiert, M. Sosnowski, K. Grabowska, A. Zylka, A. Kulakowska, D. Skrobek, S. Mistal, and Y. Gao, "CO₂ capture by virgin ivy plants growing up on the external covers of houses as a rapid complementary route to achieve global GHG reduction targets", *Energies*, vol. 15, no. 5, p. 1683, 2022.
[<http://dx.doi.org/10.3390/en15051683>]
- [2] D. Jasim, T. Mohammed, and M. Abid, "A review of the natural gas purification from acid gases by membrane", *Eng. Technol. J.*, vol. 40, no. 3, pp. 441-450, 2022.
[<http://dx.doi.org/10.30684/etj.v40i3.1983>]
- [3] G. da Cunha, J. de Medeiros, and O. Araújo, "Carbon capture from CO₂-rich natural gas via gas-liquid membrane contactors with aqueous-amine solvents: A review", *Gases*, vol. 2, no. 3, pp. 98-133, 2022.
[<http://dx.doi.org/10.3390/gases2030007>]
- [4] W.A. Poe, and S. Mokhatab, "Introduction to natural gas processing plants", In: *Modeling, Control, and Optimization of Natural Gas Processing Plants*, Elsevier, 2017, pp. 1-72.
[<http://dx.doi.org/10.1016/B978-0-12-802961-9.00001-2>]
- [5] Q. Nasir, "A hybrid membrane-absorption process for carbon dioxide capture: Effect of different alkanolamine on energy consumption", *Iran J Chem Chem Eng*, vol. 39, no. 5, pp. 239-254, 2020.
- [6] S. Murbini, "Technology challenge for Natuna gas development", In: *27th Annual Convention Proceedings*. 2000, pp. 1-13
- [7] S.E. Zanco, J.F. Pérez-Calvo, A. Gasós, B. Cordiano, V. Becattini, and M. Mazzotti, "Post-combustion CO₂ capture: A comparative techno-economic assessment of three technologies using a solvent, an adsorbent, and a membrane", *ACS Engineering Au*, vol. 1, no. 1, pp. 50-72, 2021.
[<http://dx.doi.org/10.1021/acseengineeringau.1c00002>]
- [8] H. Anselmi, O. Mirgoux, R. Bounaceur, and F. Patisson, "Simulation of post-combustion CO₂ capture, a comparison among absorption, adsorption and membranes", *Chem. Eng. Technol.*, vol. 42, no. 4, pp. 797-804, 2019.
[<http://dx.doi.org/10.1002/ceat.201800667>]
- [9] A.H. Astari, "Masela field composition", M.S. thesis, Universitas St. Stavanger, 2017.
- [10] M. Nizami, R.I. Nugroho, K.H. Milati, Y.W. Pratama, and W.W. Purwanto, "Process and levelized cost assessment of high CO₂-content natural gas for LNG production using membrane and CFZ CO₂ separation integrated with CO₂ sequestration", *Sustain. Energy Technol. Assess.*, vol. 49, p. 101744, 2022.
[<http://dx.doi.org/10.1016/j.seta.2021.101744>]
- [11] R.P. Anugraha, V.D. Pratiwi, R. Renanto, J. Juwari, A.N. Islami, and M.Y. Bakhtiar, "Techno-economic analysis of CO₂ cryogenic distillation from high CO₂ content gas field: A case study in Indonesia", *Chem. Eng. Res. Des.*, vol. 202, pp. 226-234, 2024.
[<http://dx.doi.org/10.1016/j.cherd.2023.12.035>]
- [12] X. Luo, and M. Wang, "Improving prediction accuracy of a rate-based model of an MEA-based carbon capture process for large-scale commercial deployment", *Engineering*, vol. 3, no. 2, pp. 232-243, 2017.
[<http://dx.doi.org/10.1016/j.eng.2017.02.001>]
- [13] S.S. Hosseini, and J.F.M. Denayer, "Biogas upgrading by adsorption processes: Mathematical modeling, simulation and optimization approach - A review", *J. Environ. Chem. Eng.*, vol. 10, no. 3, p. 107483, 2022.
[<http://dx.doi.org/10.1016/j.jece.2022.107483>]
- [14] B. Kottititum, T. Srinophakun, N. Phongsai, and Q.T. Phung, "Optimization of a six-step pressure swing adsorption process for biogas separation on a commercial scale", *Appl. Sci.*, vol. 10, no. 14, p. 4692, 2020.
[<http://dx.doi.org/10.3390/app10144692>]
- [15] W. Djeridi, A. Ouederni, N.B. Mansour, P.L. Llewellyn, A. Alyamani, and L. El Mir, "Effect of the both texture and electrical properties of activated carbon on the CO₂ adsorption capacity", *Mater. Res. Bull.*, vol. 73, pp. 130-139, 2016.
[<http://dx.doi.org/10.1016/j.materresbull.2015.08.032>]
- [16] C.A. Grande, "Biogas upgrading by pressure swing adsorption", In: *Biofuel's Engineering Process Technology*, InTech, 2011.
[<http://dx.doi.org/10.5772/18428>]
- [17] M.S.P. Maksimov, "Modelling of gas separations using Aspen Adsorption® software", M.S. thesis, Lahti University of Technology, 2021.
- [18] N. Wang, D. Wang, A. Krook-Riekkola, and X. Ji, "MEA-based CO₂ capture: A study focuses on MEA concentrations and process parameters", *Front. Energy Res.*, vol. 11, p. 1230743, 2023.
[<http://dx.doi.org/10.3389/fenrg.2023.1230743>]
- [19] N.F.A. Mustafa, A.M. Shariff, W.H. Tay, and S.M.M. Yusof, "Effect of carbon dioxide (CO₂) concentration in the gas feed on carbon dioxide absorption performance using aqueous potassium carbonate promoted with glycine", *E3S Web Conf*, vol. 287, no. 1, p. 02007, 2021.
[<http://dx.doi.org/10.1051/e3sconf/202128702007>]